

## Contour Dynamics: Kinetic electron simulation of collisionless reconnection

H.J. de Blank and E.V. van der Plas

*FOM-Institute for Plasma Physics Rijnhuizen,  
Association Euratom-FOM, Trilateral Euregio Cluster,  
P.O. Box 1207, 3430 BE Nieuwegein, The Netherlands, [www.rijnhuizen.nl](http://www.rijnhuizen.nl)*

**Introduction** Fast magnetic reconnection observed in near-collisionless plasmas in space and in experiments approaching fusion conditions, has motivated the study of electron inertia as a fast reconnection mechanism. In thermonuclear magnetic confinement, reconnection is of particular concern as it connects field lines that originate in plasma regions with different temperatures, thus reducing thermal insulation. In collisionless plasmas, where electrons move rapidly along the reconnecting field lines, a temperature difference poses a fundamental physics problem whose solution requires a kinetic model. Temperature gradients were shown to deform the magnetic island x-points during fast collisionless reconnection when electron inertia decouples the plasma motion from the magnetic field [1], and to deform and shift the magnetic islands in the linear and nonlinear phases of a reconnecting instability [2]. In [1, 2] a kinetic electron model describes the collisionless processes during the reconnection of field lines originating in regions with different temperatures. Here we use the same model for nonlinear numerical simulations of the reconnecting instability of an annular cylindrical current distribution. The choice of equilibrium implies that the instability is a surface mode, which enables us to use a kinetic Contour Dynamics code to describe the dynamics on the inertial scale length  $d_e$ . The strong guide magnetic field causes electrons with equal parallel velocities to move together as an incompressible fluid perpendicular to the field. We approximate the full electron distribution with a finite number of such fluids. The computed evolution of reconnecting instabilities of cylindrical symmetric current distributions show the effects of temperature differences on the magnetic island structure.

**Drift-kinetic model** The island geometry is captured in a 2D model with a strong magnetic guide field in the  $z$ -direction and perturbations that only depend on  $(x, y)$ :  $\mathbf{B} = B_0 \mathbf{e}_z + \mathbf{e}_z \times \nabla \psi$ , with  $|\nabla \psi| \ll B_0$ , in order to model a low- $\beta$  tokamak. This ordering neglects magnetic curvature and particle trapping due to  $\nabla B$ . The electric field is  $\mathbf{E} = \mathbf{e}_z \partial \psi / \partial t - \nabla \phi$  and  $\phi, \psi$  are the electric and magnetic potentials. The electrons and their velocities  $\parallel \mathbf{B}$  are described by a distribution function  $f(t, x, y, v_z)$ , where  $v_z = v_{\parallel} + e\psi/m$  is the canonical momentum. In these coordinates, the collisionless drift-kinetic equation is [1, 2, 3]

$$\frac{\partial f}{\partial t} + [\Phi, f] = 0, \quad \Phi(v_z) = \frac{1}{B_0} (\phi + v_z \psi - \psi^2 e / 2m). \quad (1)$$

if the coordinate  $z$  is ignorable. The bracket is defined as  $[g, h] = \mathbf{e}_z \cdot \nabla g \times \nabla h$ . The fields depend on  $f$  via the cold ion vorticity equation and Ampère's law,

$$n + \nabla^2 \phi / (e v_A^2) = \int f dv_z, \quad (\nabla^2 - d_e^{-2}) \psi = -e \int f v_z dv_z. \quad (2)$$

Here  $d_e = \sqrt{m/e^2 n}$  is the inertial skin depth and  $v_A = B_0/\sqrt{m_i n}$  the Alfvén velocity.

**Contour Dynamics** In order to apply the contour dynamics method, we divide the electron velocity distribution function into a time-independent Maxwellian distribution for the bulk electrons and a smaller time-dependent part that we discretize in velocity space,

$$f(x, y, v_z, t) = \frac{n}{v_t \sqrt{\pi}} e^{-v_z^2/v_t^2} + \sum_{i=0}^{N-1} f_i(t, x, y) \delta(v_z - v_i). \quad (3)$$

With this discretization, the drift-kinetic equation (1) reduces to  $N$  evolution equations

$$\frac{\partial f_i}{\partial t} + [\Phi(v_i), f_i] = 0, \quad (4)$$

governed by  $N$  different stream functions  $\Phi(v_0), \dots, \Phi(v_{N-1})$ . Solving Eqs. (2) for small  $\phi$  and  $\psi$ , we obtain these stream functions for every parallel velocity  $v_z$  as integrals over the distribution function  $f(\mathbf{x}, v_z, t)$  with a Green's function  $G$ ,

$$\Phi(\mathbf{x}, v, t) = \int_C d^2 x' \int_{-\infty}^{\infty} dv' G_{vv'}(|\mathbf{x} - \mathbf{x}'|) f(\mathbf{x}', v', t), \quad G_{vv'}(r) \equiv \frac{1}{2\pi} \left( \ln r + \frac{vv'}{v_A^2} K_0\left(\frac{r}{d_e}\right) \right). \quad (5)$$

Here  $K_0$  is the modified Bessel function of the second kind.

We also assume that each function  $f_i(\mathbf{x}, t)$  is constant in a region  $C_i$  bounded by a closed contour  $\partial C_i$ . Then, according to Eqs. (4), the evolution of  $f_i(\mathbf{x}, t)$  is completely described by the motion of the contour  $\partial C_i$  in the  $x$ - $y$  plane. The contour velocities can be obtained by substituting the discretized distribution function (3) in (5) and to use Stokes' theorem to describe the velocity of the  $j$ -th contour as a sum of line integrals around all contours,

$$\Phi_j(\mathbf{x}, t) = \sum_{i=1}^N f_i \int_{C_i(t)} d^2 x' G_{v_i v_j}(|\mathbf{x} - \mathbf{x}'|), \quad \mathbf{v}_j(\mathbf{x}, t) = - \sum_{i=1}^N f_i \oint_{\partial C_i(t)} d\mathbf{x}' G_{v_i v_j}(|\mathbf{x} - \mathbf{x}'|).$$

Thus the kinetic dynamics is reduced to interactions between 2-D contours.

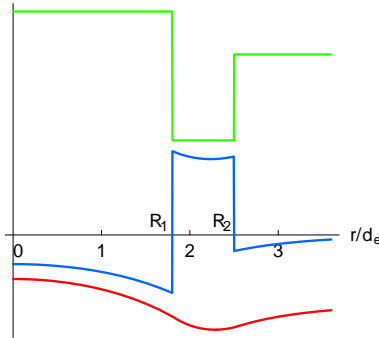


*Fig. 1. Equilibrium with an annular current distribution ( $\nabla^2 \psi$ ) between  $R_1$  and  $R_2$  (blue line), that is shielded on a length scale  $d_e$ . The green line shows the  $x$ -dependence of the electron distribution  $f_i$  and  $d_e^{-2} \psi - \nabla^2 \psi$ , and the red line is  $\psi(r)$ .*

**Equilibrium** We consider the stability of a current-annulus, at  $R_1 < R < R_2$  in cylinder coordinates. This current distribution is described by contours that are  $N$  circles with radius  $R_1$  and  $N$  circles with radius  $R_2$ . The  $j$ th moment of the distribution is  $n_j = (v_t/2)^j \int f(v_z) H_j(v_z/v_t) dv_z$ , where  $H_j$  is a Hermite polynomial. For the discretization velocities  $v_i$  we choose the  $N$  zeros of the  $N + 1$ th Hermite polynomial,  $H_N(v_i/v_t) = 0$ . Thus, we describe the lowest  $N$  moments

$n_0, \dots, n_{N-1}$ , while the next moment vanishes ( $n_N = 0$ ). In the present simulations, the weights  $f_i$  are chosen so that initially only the current ( $-en_1$ ) and the temperature perturbation ( $mn_2/n$ ) are nonzero while the remaining moments  $n_0, n_3, \dots, n_{N-1}$  vanish. The weights of the contours at  $R = R_1$  and  $R = R_2$  determine the jumps in the current density. They are chosen such that a mode with given poloidal mode number  $m$  is unstable. A typical distribution is shown in Fig. 1. Reconnection starts at the position  $d\psi/dr = 0$  between  $R_1$  and  $R_2$ .

**Numerical results** The  $2N$  contours are given an initial  $e^{im\theta}$  perturbation of  $10^{-3}d_e$  and are evolved with a code that generalizes to the kinetic model ( $N \geq 4$ ) a symplectic contour area preserving code [4] for a 2-D Eulerian fluid ( $N = 1$ ). A version [5] with  $N = 2, 3$  models the isothermal two-fluid plasma [6]. Simulations with  $N = 5, 7, 10$  show convergence of the current density and temperature perturbations. Here we show  $N = 10$  results. The growth of an  $m = 3$

Fig. 2. Evolution of  $\psi$  (top) and the temperature distributions (bottom) during an  $m = 3$  reconnecting instability. The initial jumps in the temperature and current density are at  $R_1 = 4.0d_e$  and  $R_2 = 5.5d_e$ .

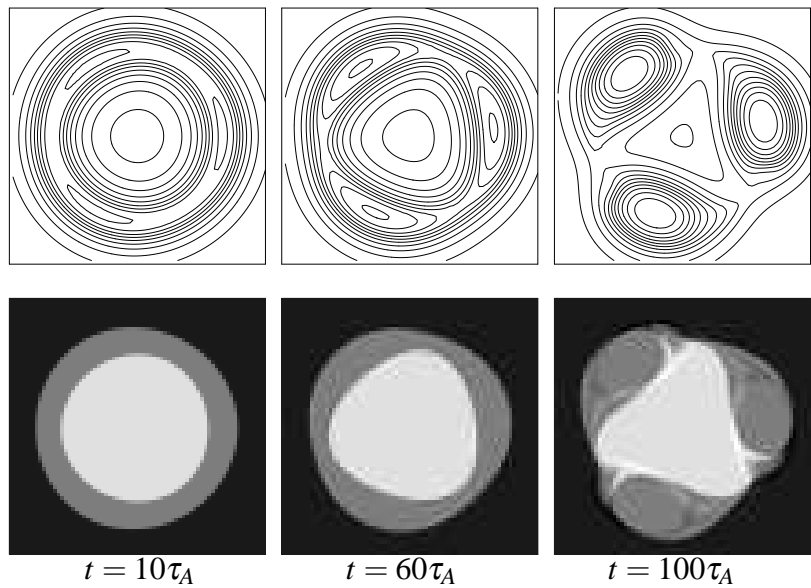
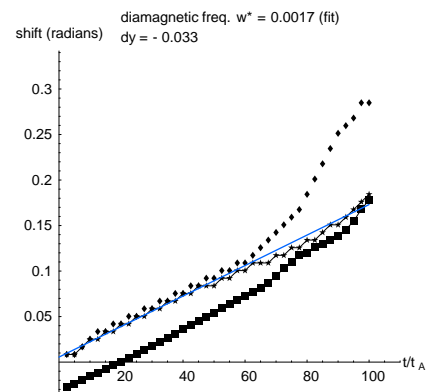


Fig. 3. Time dependence of the poloidal angles of the x-point (diamonds), the o-point ( $\theta_O$ , stars), and the phase angle of the external perturbations (squares), corresponding to  $\psi$  in Fig. 2. The straight line is a fit of  $\theta_O$  in the time interval where the mode is approximately linear, i.e. before saturation. The slope gives an effective  $\omega_* = 1.68 \times 10^{-3} s^{-1}$ .



mode is shown in Fig. 2. In the nonlinear stage (e.g. at  $t = 100\tau_A$ ) the magnetic islands are no longer mirror-symmetric. This is a consequence of the temperature gradients. The sloped line in Fig. 3 show that the mode rotates with the electron diamagnetic frequency. When the magnetic islands become sufficiently wide, the x-point temperature gradient becomes much higher than the o-point gradient, so that the x-points rotate faster than the o-points (Fig. 3), deforming the islands. Without temperature gradients, the islands would be mirror-symmetric. Both linearly

and nonlinearly, the magnetic islands have a poloidal phase shift with respect to the far fields. A similar result was found analytically for reconnecting instabilities of a straight plasma slab [2].

Fig. 4. Dependence of the  $x$ -point shape on the ratio  $v_t/v_A = \rho_s/d_e$ . The colored lines are contours with  $v_i \approx \pm v_t$ . The black line is the magnetic separatrix.

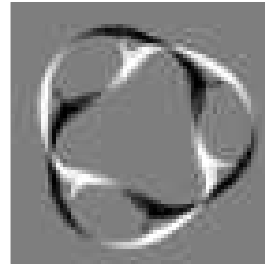
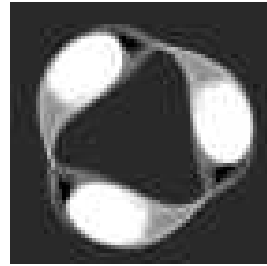
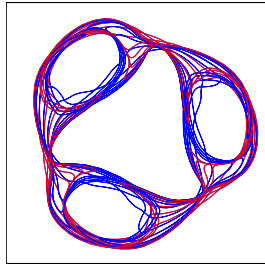
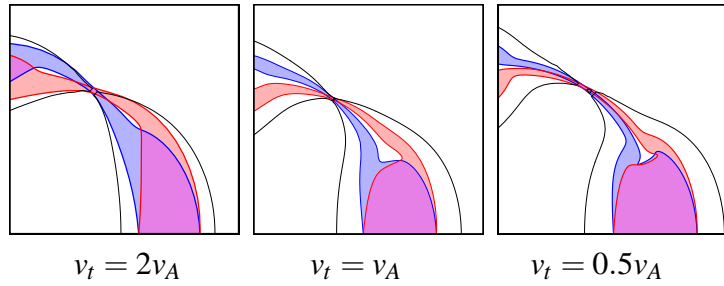


Fig. 5. Left: the  $2 \times 10$  contours, containing complete information of the plasma at  $t = 100\tau_A$ ; center: current density; right: electron density, all at  $t = 100\tau_A$ .

Fig. (4) shows the separatrix (black line) near an  $x$ -point for three values of the ratio  $v_t/v_A$ . For small values of  $v_t$ , the  $x$ -point angle is small since slow electrons are advected by a stream function  $\Phi \approx \phi$ . Faster electrons tend to follow the field lines ( $\Phi \approx v_z \psi$ ). The contours (colored lines) show this. They also show the formation of very small scales ( $\ll d_e$ ) near the  $x$ -point. In an isothermal 2-fluid model ( $N = 2$ ) this leads to equally small scales in the current density, at least in slab geometry [1]. However, a kinetic model broadens the  $x$ -point current layer, illustrated by the thermal spread of the contours in Fig. 5. Indeed, the corresponding current density distribution (Fig. 5, center) has a finite width in the  $x$ -points. The right frame of Fig. 5 shows the perturbation of the density, which is proportional to the vorticity  $\nabla^2 \phi$ .

Note that the contour model includes the linear effects of Landau damping, whereas nonlinearly, a damping mechanism is not immediately evident since the model does not permit explicit phase mixing in velocity space. However, this mixing in velocity space is replaced by spatial mixing: numerically, one finds the development of increasingly small scales (see also [3]). Essential is the fact that contours with different  $v_i$  develop different small scales.

**Acknowledgement** This work, supported by the European Communities under the contract of Association between EURATOM/FOM, was carried out within the framework of the European Fusion Programme with financial support from NWO. The views and opinions expressed herein do not necessarily reflect those of the European Commission.

## References

- [1] H. J. de Blank and G. Valori, Plasma Phys. Control. Fusion **45** (2003) A309.
- [2] E.V. van der Plas and H.J. de Blank, Phys. Rev. Lett. **98** (2007) 265002.
- [3] T. V. Liseikina, F. Pegoraro and E. Yu. Echkina, Phys. Plasmas **11** (2004) 3535.
- [4] P. W. C. Vosbeek and R. M. M. Mattheij, J. Comput. Phys. **133** (1997) 222.
- [5] J. H. Mentink, J. Bergmans, L.P.J. Kamp, and T.J. Schep, Phys. Plasmas **12** (2005) 052311.
- [6] T. J. Schep, F. Pegoraro and B. N. Kuvshinov, Phys. Plasma **1** (1994) 2843.